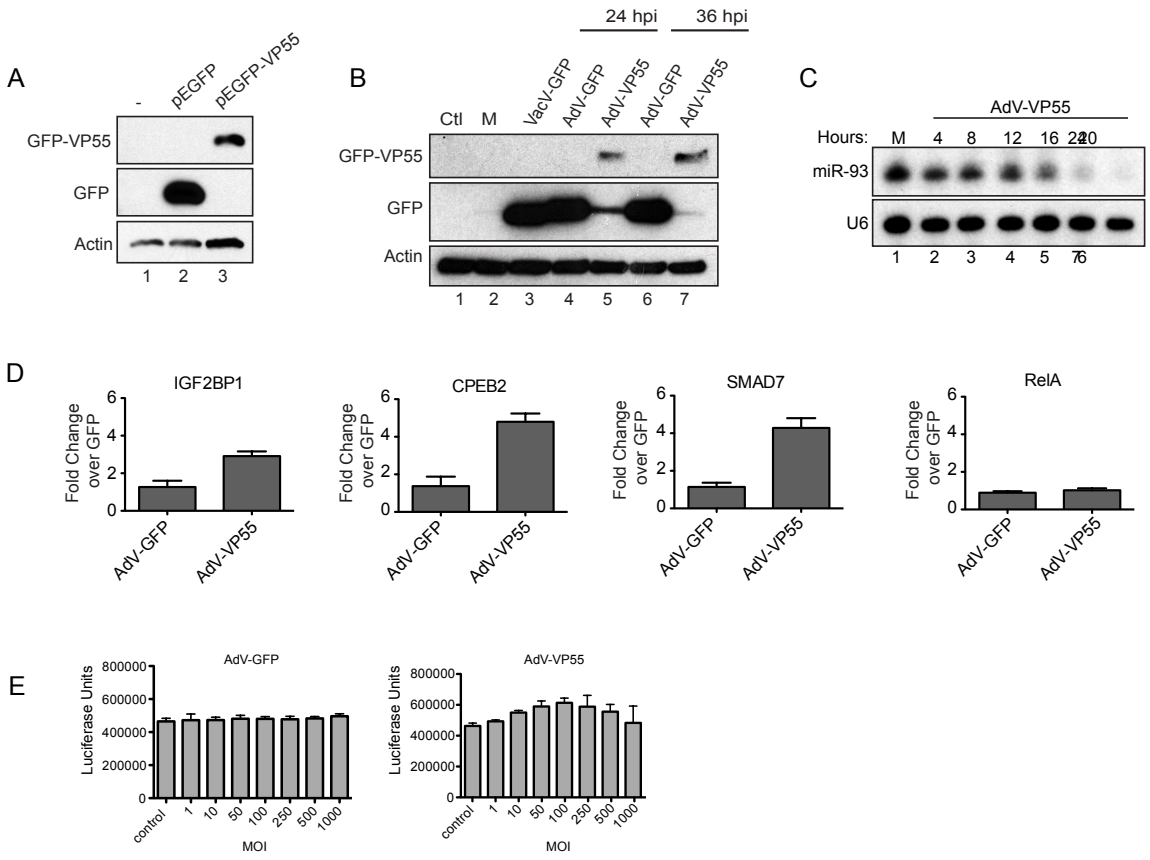

Supplemental Figure 1. Characterization of pEGFP-VP55 and Adenoviral vectors. Related to Figure 1.
(A) Western blot for EGFP expression in NoDice cells transfected with either pEGFP or pEGFP-VP55 for 24hrs. (B) Western blot for EGFP expression of 293T cells treated with Vaccinia-GFP, AdV-GFP, or AdV-VP55 at the indicated time points. (C) Small RNA northern blot of 293T cells treated with AdV-VP55 for the indicated time points. (D) qPCR of 293T cells treated with AdV-GFP or AdV–VP55 for 24 hrs for indicated genes. (E) CellTiterGlo Assay of 293T cells treated with AdV-GFP or AdV-VP55 at indicated MOIs 24hrs post-transduction.

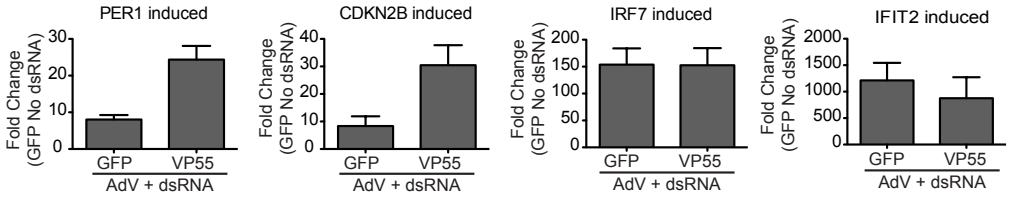

Supplemental Figure 2. Validation of deep sequencing results from immortalized fibroblasts and primary fibroblasts treated with dsRNA. Related to Figure 2.

qPCR of BJ cells treated with AdV-GFP or AdV-VP55 for 24 hrs prior to transfection with dsRNA. Total RNA collected 6hrs post-transfection. All samples were normalized to tubulin. Fold changes over samples treated with AdV-GFP alone. Error bars denote ± SD.

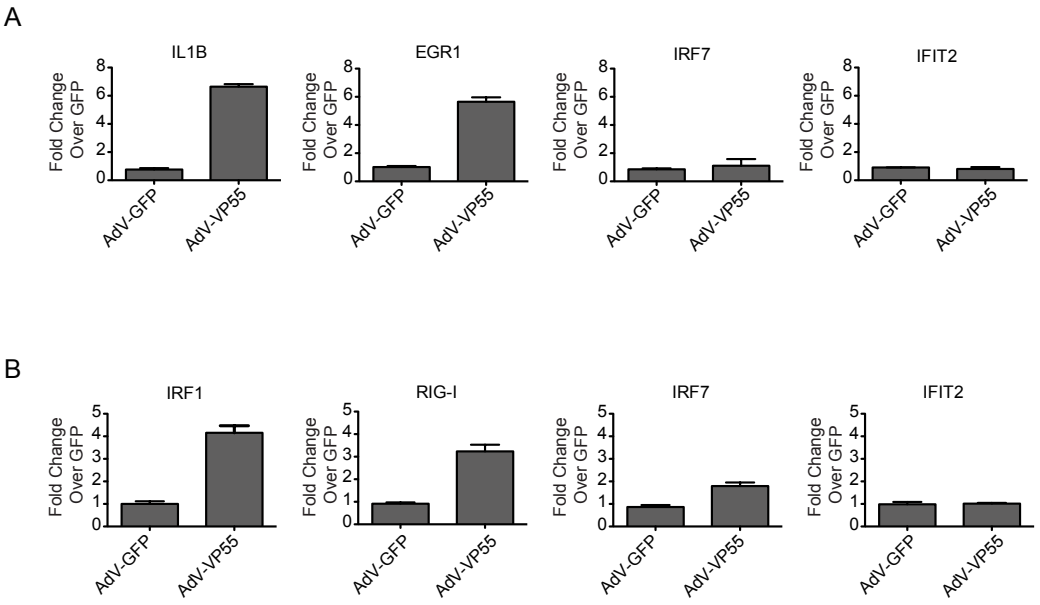

Supplemental Figure 3. Validation of deep sequencing results from Adeno vector-treated primary fibroblasts. Related to Figure 3.

qPCR of BJ fibroblasts treated with AdV-GFP or AdV–VP55 for 24 hrs (A) or 9 days (B) for indicated genes. All samples were normalized to tubulin. Fold changes over samples treated with AdV-GFP alone. Error bars denote ± SD.

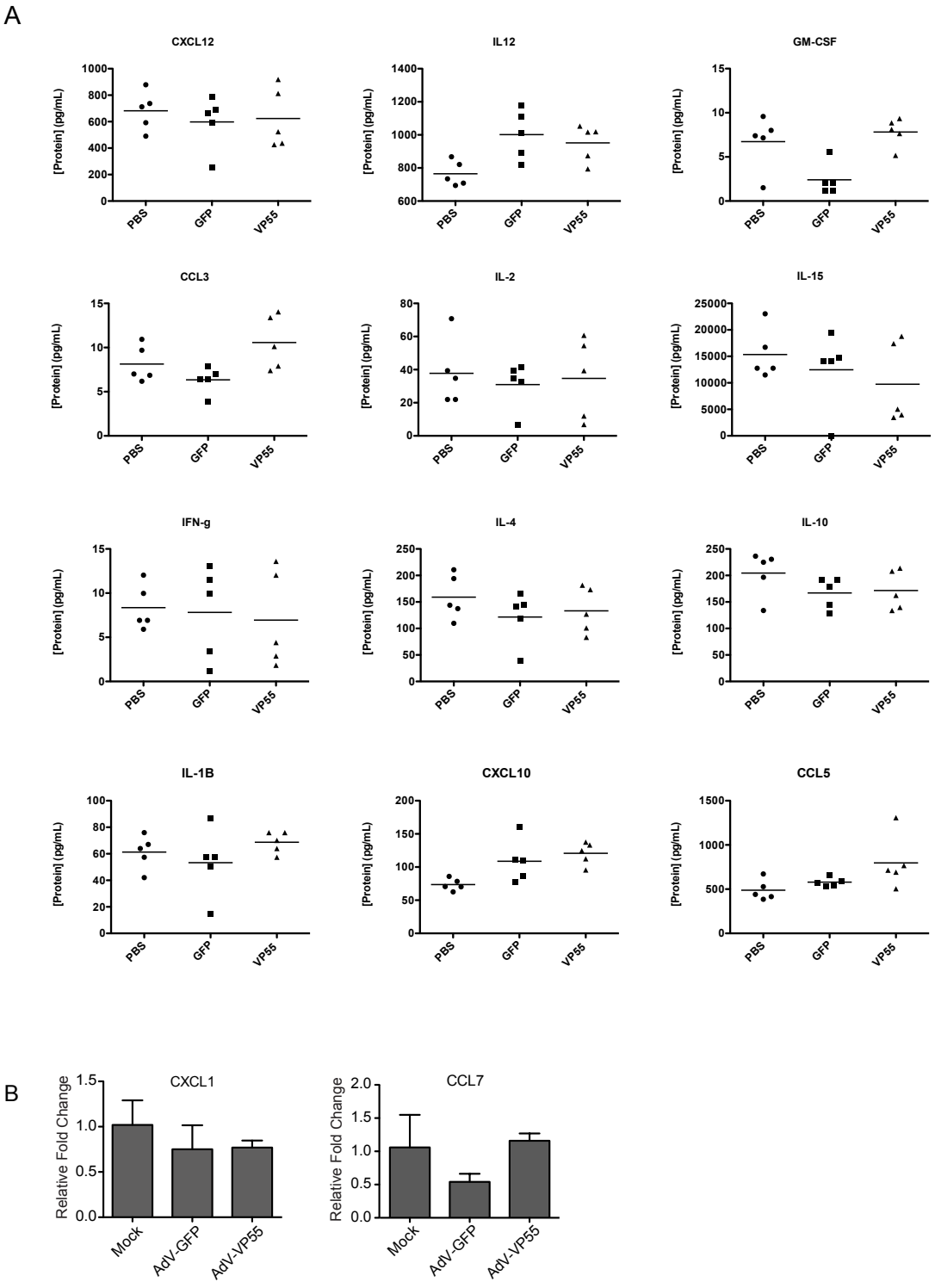

Supplemental Figure 4. Characterization of the cytokine response to loss of miRNA silencing *in vivo*. Related to Figure 4.

(A) Cytokine concentrations from mice treated in Figure 4A. Graphs depict cytokines that were detectable in the assay, but not significantly altered across treatment conditions. Significance was determined using an one-tailed Student's *t* test. p-values < 0.05 were considered statistically significant. (B) qPCR of RNA from lungs in Figure 4A for indicated genes. All samples normalized to tubulin. Fold change over mock-treated cohort.

SUPPLEMENTAL TABLE LEGENDS

Table S1. Small RNA and mRNA analysis of immortalized fibroblasts transfected with pEGFP-VP55 or infected with Adenoviral vectors. Related to Figure 1.
mRNA-Seq analysis of NoDice cells transfected with pEGFP or pEGFP-VP55 for 24hrs and small RNA and mRNA-Seq analysis of 293T cells mock treated or treated with either AdV-GFP or AdV-VP55 for 24 hours. Table contains the gene symbol, read status, mean read count, $\log_2$ fold change, standard error of the $\log_2$ fold change, and the multiple-testing adjusted p-value (q value) for all genes detected in the experiments and additional tabs contain the subsets of genes determined to be differentially expressed ($q<0.05$). Tab for small RNA deep sequencing contains the name, sequence, read numbers for each condition, and fold changes for annotated mature miRNAs.

Table S2. Transcriptome profiling of dsRNA- or IFNβ-treated primary fibroblasts in the presence or absence of endogenous miRNAs. Related to Figure 2.
Analysis of BJ fibroblasts treated with AdV-GFP of AdV-VP55 for 24 hours prior to mock, dsRNA transfection for 6 hours, or IFNβ treatment for 6 or 24 hours prior to mRNA-Seq. Table contains the gene symbol, read status, mean read count, $\log_2$ fold change, standard error of the $\log_2$ fold change, and the multiple-testing adjusted p-value (q value) for all genes detected in the experiments. Additional tabs contain the subsets of all genes that were differentially expressed ($q<0.05$) as well as the subsets of differentially expressed genes that were also induced 2-fold or more for each experimental condition.

Table S3. Transcriptome profiling of miRNA depleted primary fibroblasts.
Related to Figure 3.
Analysis of BJ fibroblasts treated with AdV-GFP or AdV-VP55 for 24 hours or 9 days prior to mRNA-Seq. Table contains the gene symbol, read status, mean read count, $\log_2$ fold change, standard error of the $\log_2$ fold change, and the multiple-testing adjusted p-value (q value) for all genes detected in the experiment. Additional tabs contain the subsets that were differentially expressed ($q<0.05$) and the subsets of differentially expressed genes that were induced 2-fold or more for each time point.

Table S4. Transcriptome profiling and pathway prediction analysis of differentially expressed genes in AdV-GFP and AdV-VP55-treated whole lung tissue. Related to Figure 4.
mRNA Seq analysis of whole lung tissue from mice treated intranasally with 2.5×10^8pfu of AdV-GFP or AdV-VP55 for 48 hours. Table contains the gene symbol, read status, mean read count, $\log_2$ fold change, standard error of the $\log_2$ fold change, and the multiple-testing adjusted p-value (q value) for all genes detected in the experiment. Subsequent tabs contain the subset determined to be differentially expressed ($q<0.05$), differentially expressed genes from AdV-VP55 murine lung tissue up- or down-regulated by $\log_2$ 2-fold or more, and the ConsensusPathDB interaction database output for the ten most significant categories from the over-representation analysis of induced genes (in black) and the four most significant categories for repressed genes (red).

SUPPLEMENTAL MATERIAL AND METHODS

Cell Culture, Tranfections, and Reagents

HEK 293T, HEK 293T Dicer -/- (NoDice) (Bogerd et al., 2014), and primary human foreskin fibroblasts (BJ (ATCC CRL-2522)) were maintained in Dulbecco's modified Eagle's medium (DMEM) supplemented with 10% (vol/vol) fetal bovine serum (FBS) and 1% penicillin-streptomycin at 37°C and 5% CO_2. All plasmid transfections were performed in OptiMem (Life Technologies) +10% FBS using Lipofectamine 2000. IFNB (BEI Resources) was used at a final concentration of 350units/mL. poly(I:C) (Sigma) was transfected at 0.8µg/mL final volume in OptiMem (Life Technologies) +10% FBS using Lipofectamine 2000 (Invitrogen) as per the manufactures instructions. mmu-let-7f and hsa-miR-23a-3p miRIDIAN miRNAmimics (Dharmacon) were transfected at a final concentration of 13nM either alone in OptiMem + 10% FBS using Lipofectamine RNAiMAX Transfection Reagent (Invitrogen) as per the manufactures instructions or in combination with plasmids as described above.

Small RNA Deep Sequencing

Small RNA deep sequencing was performed as previously described (Pfeffer et al., 2005). Briefly, 10µg of total RNA was separated on a 12% denaturing Tris-Urea gel. The ~19-24nt size fraction was excised, purified, and ethanol precipitated. The 3' linker was ligated using T4RNA ligase2, truncated (NEB). RNA was again fractioned and purified. The 5' linker was then ligated using T4 RNA ligase (Ambion) followed by another round of size fractionation, purification, and precipitation. Both 3' and 5' linkers have randomized ends with four random nucleotides (N) at the insertion site to reduce ligase bias (Jayaprakash et al., 2011). RNA containing both the 3' and 5' linkers was then reverse transcribed using SuperScript III (Invitrogen). PCR amplification of cDNA was performed using OneTaq 2x PCR Master Mix (NEB) and barcoded reverse primer for multiplexed sequencing. Sample size and concentration was assessed by Bioanalyzer DNA1000 assay prior to sequencing on an Illumina HiSeq 2500 platform for 100nt single end reads. Linker sequences were removed from raw reads, consolidated, and then aligned to human annotated miRNA sequences using Bowtie in addition to custom Python scripts. Raw read numbers were used directly as an internal control (reads matching to U1 small nuclear RNA) were comparable measuring 23,734 reads in response to AdV-GFP and 30,626 reads in response to AdV-VP55. Adenovirus specific reads in this small RNA sample were 158 reads in response to AdV-GFP and 106 in response to AdV-VP55. The raw data are available under the accession numbers: GSM1909499, GSM1909500, GSM1909501

RNA Analysis

Total RNA was isolated using TRIzol (Invitrogen) according to the manufactures protocol. Small RNA northern blotting was performed using 10µg of 293T or 2µg of BJ total RNA as previously described (Pall and Hamilton, 2008). Probes used included anti-U6 5'- GCCATGCTAATCTTCTCTGTATC-3', anti-let-7 5'-AACTATACAACCTACTACCTCA-3', anti-miR-93 5'- CTACCTGCACGAACAGCACTT, and anti-miR-20 5'-CTACCTGCACTATAAGCACTTTA-3'.

Reverse transcription for qRT-PCR was performed using SuperScript II with oligo-dT primers according to manufactures protocols. cDNA was amplified using primers specific for tubulin, IL6, IRF7, IFIT2, IRF1, EGR1, EGR2, IGF2BP1, CPEB2, SMAD7, RelA, PER1, CDKN2B, IL1β, RIG-I, CCL2, CCL4, CCL7, CXCL1, and EGFP with KAPA SYBR FAST qPRC Master Mix (KAPA Biosystems) and analyzed on a CFX96 Real-Time System (BioRad) or a LightCycler 480 (Roche).

Determination of *in vivo* cytokine levels

Whole lungs were extracted 48hrs post-transduction. Protein levels of cytokines/chemokines in whole lung tissue were assessed using a multiplexed bead array assay as previously described (Heaton et al., 2014). Briefly, whole lung tissue was homogenized in 700µL PBS supplemented with protease inhibitor. For each cytokine assayed, 1,500 cytokine-specific antibody-conjugated capture beads were used in a total volume of 50µL. Plates were read on a Luminex MAGPIX platform. At least 50 beads per cytokine were recorded and the median fluorescence intensity was analyzed with Milliplex software using a 5P regression algorithm.

Determination of *in vivo* RNA levels

Whole lungs were extracted 48hrs post-transduction and initially processed as described above. After removal of all supernatant from the initial homogenization, remaining solid tissue was homogenized again in 1mL Trizol reagent. RNA was then extracted according to manufactures protocol. 1µg of total RNA was then used for mRNA seq and qPCR as described above.

Luciferase Assays
Gaussia luciferase reporter constructs were engineered to contain either (1) two tandem sites perfect complementary to let-7-f, (2) a scrambled sequence of equal length, (3) the human IRF1 3'UTR (NM_002198.2, nts 1256-1971), (4) the human IRF1 3'UTR with nt substitutions in the miR-23 target site (Liu et al., 2013), (5) the human IL6 3' UTR (NM_000600, nts 756-1182), or (6) the human IL6 3'UTR with nt substitutions in the let-7 target site (Iliopoulos et al., 2009). For assessment of post-transcriptional silencing in the presence of VP55, HEK 293T cells were transfected as described above with (1) either let-7 targeted or scrambled Gaussia luciferase constructs, (2) pEGFP or pEGFP-VP55, and (3) an untargeted Firefly luciferase to normalize for transfection efficiency. Twenty-four hours post transfection, the transfection media was replaced with complete DMEM. Luciferase expression was analyzed 4 hours later. For validation of endogenous miRNA target sites, NoDice cells were co-transfected with (1) Gaussia luciferase constructs containing the 3'UTRs of either IRF1, IL6, or the control in which the putative miRNA target site was mutated, (2) an untargeted Firefly luciferase to normalize for transfection efficiency, and (3) the respective miRNA mimetic. Forty-four hours post-transfection, the transfection media was replaced with complete DMEM. Luciferase expression was analyzed 4 hours later. In all experiments Gaussia luciferase expression was normalized to Firefly.

Gene Ontology Analysis
To determine the general function of differentially expressed genes following AdV-VP55 administration in vivo, we utilized the gene lists that were found to be greater or less than a log2 fold change of two when compared to AdV-GFP. Gene lists of 139 and 138, respectively, were used as input in the gene set analysis suite software consensuspathdb.org. Using their over-representation analysis algorithm, gene symbol IDs were used and compared against Gene ontology categories for which we limited our output to biological processes for level 4 categories. Ontology categories shared by more than 25 genes are connected. The ten most significant categories were depicted for genes induced in response to VP55 with the removal homotypic cell:cell adhesion due to the extensive overlap with the ontology category for leukocyte cell-cell adhesion. The same methodology was applied for genes down regulated in response to VP55.

Cell Viability Assay
Adeno vector toxicity was determined 24hrs post-AdV transduction using CellTiter-Glo Luminescent Cell Viability Assay (Promega) according to the manufactures protocol.

Western Blotting
Cells were lysed in RIPA buffer supplemented with protease inhibitor and PMSF. Protein extracts were separated on a 4-15% Mini-PROTEAN TGX polyacrylamide gel (BioRad), transferred to a nitrocellulose membrane (BioRad), and blocked in 5% milk for one hour. Membranes were then incubated with the indicated antibodies diluted in 5% milk. Rabbit anti-EGFP (SC-8334, Santa Cruz Biotechnology) was used at 1:500, rabbit anti-IRF-1(C-20) (SC-497, Santa Cruz Biotechnology) was used at 1:200, anti-pan-actin (Neomarkers) was used at 1:2000, and secondary mouse and rabbit HRP-conjugated antibodies (GE Healthcare) were used at a 1:5000 dilutions. Immobilon Western Chemoluminescent HRP substrate (Millipore) was used for antibody detection according to the manufacture's instructions.

Statistical Analysis
Statistical analysis was performed using one-tailed Student's *t* test. p-values < 0.05 were considered statistically significant.

qPCR Primers

Target Gene	Species	Forward primer (5' to 3')	Reverse primer (5' to 3')
IL-6	human	GGTCAGAAACCTGTCCACTG	CAAGAAATGATCTGGCTCTG
IRF7	human	GGTGTGTCTTCCCTGGATAG	GCTCCAGCTCCATAAGGAAG
IFIT2	human	CGTGGGAACCTGGTGACTAA	TCGTTCCAAGCATACCGTGA
IRF1	human	CAACATGCCCATCACTCGGA	TTGATGTCCCAGCCATGCTT
EGR1	human	TGTGTCAGAGTGTTGTTCCG	AACATACAAAAATCGCCGCC
EGR2	human	TCCCAGGCTCAGTCCAACCCC	ACGGCCTTGGCGGTCATCAT
IGF2BP1	human	CAGTTCTTGGTCAAATCCGGC	CCAGTACTTCCCATCGGAGC
CPEB2	human	GGCCATTAAGGGCTGTGGAA	AGCTGAACAAACCGAGCACT
SMAD7	human	CCTCGGAAGTCAAGAGGCTG	TCTGGACAGTCAGTTGGTTTGA
RelA	human	AGCTTGTAGGAAAGGACTGCC	TTGTTGGTCTGGATGCGCT
PER1	human	GGAGCTTCCACTCGGCTG	GCTTGGCTGAGGGAGTGAG
CDKN2B	human	AGGCGCGCGATCCAG	CATCATGCACCGGTCGGG
IL1B	human	AGATGAAGTGCTCCTTCCAGG	CATGGCCACAACAACTGACG
RIG-I	human	AAAGCCTTGGCATGTTACAC	GGCTTGGGATGTGGTCTACT
CCL2	mouse	TTAAAAACCTGGATCGGAACCAA	GCATTAGCTTCAGATTTACGGGT
CCL4	mouse	AACCTAACCCCGAGCAACAC	GGGTCAGAGCCCATTGGTG
CCL7	mouse	CCCTGGGAAGCTGTTATCTTCAA	AGGCTTTGGAGTTGGGGTTT
CXCL1	mouse	GCACCCAAACCGAAGTCATA	CTTGGGGACACCTTTTAGCA
EGFP		GAACGGCATCAAGGTGAACTTC	CTGGGTGCTCAGGTAGTGGTTG
Tubulin	human	GCCTGGACCACAAGTTTGAC	TGAAATTCTGGGAGCATGAC
Tubulin	mouse	TGCCTTTGTGCACTGGTATG	CTGGAGCAGTTTGACGACAC

Human Codon Optimized VP55 Sequence

> [co-vp55 - 1460 bp]

AAGAATTCTACCATGAACAGAAATCCCGACCAGAACACACTGCCAAACATCACACTGAAGATTATCGAAACC
TACCTGGGGCGGGTGCCATCCGTCAACGAGTACCACATGCTGAAGCTGCAGGCAAGGAACATCCAGAAGATT
ACCGTGTTCAACAAGGACATCTTTGTGTCTCTGGTCAAGAAAAATAAGAAAAGGTTCTTTAGTGATGTGAACA
CATCCGCCTCTGAGATCAAGGACAGGATCCTGAGCTATTTCTCCAAACAGACACAGACTTACAACATCGGCA
AGCTGTTTACAATCATTGAACTGCAGTCCGTGCTGGTCACCACATATACAGATATCCTGGGAGTGCTGACTAT
TAAGGCCCCCAATGTGATCAGCTCCAAAATTTCATACAACGTGACTAGCATGGAGGAACTGGCTCGGGATAT
GCTGAACAGCATGAATGTGGCAGTCATCGACAAGGCCAAAGTGATGGGGCGCCACAATGTCTCTAGTCTGGT
GAAGAACGTCAACAAGCTGATGGAGGAATATCTGAGGAGACATAACAAGAGCTGCATCTGTTACGGAAGTT
ATTCACTGTACCTGATCAACCCTAATATTAGATACGGGGACATCGATATTCTGCAGACCAATTCCCGGACATT
CCTGATCGACCTGGCCTTCCTGATCAAGTTCATCACCGGCAACAATATCATTCTGTCTAAGATCCCATATCTGC
GAAACTACATGGTCATCAAGGACGAGAACGATAATCACATCATTGATAGTTTCAACATCCGCCAGGACACAA
TGAATGTGGTCCCCAAGATCTTTATTGATAACATCTACATCGTGGACCCTACTTTCCAGCTGCTGAACATGAT
CAAGATGTTTAGCCAGATTGACAGACTGGAGGATCTGTCCAAGGACCCAGAAAAATTCAACGCCCGGATGGC
TACCATGCTGGAGTATGTGCGCTACACACATGGCATCGTCTTTGACGGAAAGCGCAACAATATGCCCATGAA
GTGCATCATCGATGAAAACAACCGAATCGTGACAGTCACTACCAAGGACTATTTCTCCTTTAAGAAATGTCTG
GTGTACCTGGATGAGAATGTCCTGTCAAGCGACATCCTGGATCTGAACGCCGATACTTCTTGCGACTTCGAAT
CTGTGACCAACAGTGTCTATCTGATCCACGACAACATCATGTACACTTACTTCAGTAACACCATCCTGCTGTC
AGATAAGGGGAAAGTGCACGAGATCTCAGCTCGGGGCCTGTGCGCACATATTCTGCTGTATCAGATGCTGAC
TAGCGGAGAATACAAGCAGTGTCTGTCCGATCTGCTGAACTCTATGATGAATCGAGACAAAATCCCTATCTAC
TCTCATACCGAGAGGGACAAAAAGCCAGGGCGGCACGGATTCATCAACATCGAAAAGGACATTATCGTCTTC
TGAGGTACCAA

Features :

KpnI : [1453 : 1458]

EcoRI : [3 : 8]

Start : [13 : 15]

SUPPLEMENTAL REFERENCES

Bogerd, H.P., Whisnant, A.W., Kennedy, E.M., Flores, O., and Cullen, B.R. (2014). Derivation and characterization of Dicer- and microRNA-deficient human cells. Rna.

Heaton, N.S., Langlois, R.A., Sachs, D., Lim, J.K., Palese, P., and tenOever, B.R. (2014). Long-term survival of influenza virus infected club cells drives immunopathology. J Exp Med *211*, 1707-1714.

Iliopoulos, D., Hirsch, H.A., and Struhl, K. (2009). An epigenetic switch involving NF-kappaB, Lin28, Let-7 MicroRNA, and IL6 links inflammation to cell transformation. Cell *139*, 693-706.

Liu, X., Ru, J., Zhang, J., Zhu, L.H., Liu, M., Li, X., and Tang, H. (2013). miR-23a targets interferon regulatory factor 1 and modulates cellular proliferation and paclitaxel-induced apoptosis in gastric adenocarcinoma cells. PLoS One *8*, e64707.

Pall, G.S., and Hamilton, A.J. (2008). Improved northern blot method for enhanced detection of small RNA. Nat Protoc *3*, 1077-1084.